# Nonlinear dynamics in a double-chain model of DNA

K. Forinash
*Indiana University Southeast, New Albany, Indiana 47150*

A. R. Bishop and P. S. Lomdahl
*Los Alamos National Laboratory, Los Alamos, New Mexico 87545*
(Received 17 October 1990)

We investigate numerically the mechanics of a simple lattice model of DNA. The model consists of two linear-mass chains connected by a Morse potential representing the hydrogen bonding between the sugar-phosphate backbones. Effects on discrete breather-type solutions caused by random noise and mass defects, representing interaction with the local environment, are studied.

## I. INTRODUCTION

Although an understanding of the chemical changes involved in transcription and replication of DNA and RNA rests on fairly secure footing,[1] the dynamics of these processes are still being examined. This is due in part to the complexity of the problem and the probability that nonlinear vibrational modes are somehow involved.[2] Several rather simple models have been proposed[3–6] which seek to explain the open states of DNA and RNA as nonlinear excitations along the chain which stretch or even break the hydrogen bonding between the sides of the chain. Although it is not established that open states of DNA initiate transcription or replication, since open states appear randomly along chains which are not replicating, it does seem plausible that open states do play some nucleative role in the replication process, especially in the melting regime. Improvements have been made in many of these models as additional complications such as more realistic potentials and discreteness effects are taken into account. One such model which has met with some success in predicting a correct melting temperature for DNA using reasonable bonding parameters as input is due to Peyrard and Bishop.[7] They examined the statistical mechanics of a model consisting of two chains of masses connected linearly along their length and connected via a Morse potential between the two chains. This paper investigates the dynamics of their model by numerical simulation. In addition, the effects of various mass defects representing interaction of the chain with its surroundings are studied. Additional studies along these lines, including finite-temperature effects, may be found in Refs. 8–10.

In Sec. II the model and details of the simulation are discussed. Solutions for the model using the technique outlined by Remoissenet[11] for a discrete chain are considered in Sec. III along with questions of stability. Single mass defects are introduced into the model in Sec. IV and the effect these defects have on coherent anharmonic phonon ("breather") solutions are examined. Similar studies are done for multiple mass defects in Sec. V. The final section summarizes the results of the previous sections.

## II. THE MODEL

The model consists of two chains of masses connected by linear springs along their length with the addition of nonlinear coupling between masses of each chain (Fig. 1). The Hamiltonian for the system is

$$H=\Sigma_n \tfrac{1}{2}m(u_n'^2+w_n'^2)+\tfrac{1}{2}k[(u_n-u_{n-1})^2 +(w_n-w_{n-1})^2]+V(u_n-v_n)\ , \tag{1}$$

where $u$ is the top chain displacement from equilibrium and $w$ is the bottom chain displacement. Here $k$ represents the linear coupling strength along the top and bottom chains. The corresponding velocities are $v'$ and $w'$. The Morse potential was chosen to represent the (multiple) interchain hydrogen bonding for the model DNA:

$$V(u_n-w_n)=D\{\exp[-a(u_n-w_n)]-1\}^2\ . \tag{2}$$

The parameters $a$ and $D$ were chosen to correspond to realistic values for the interchain hydrogen bond in the DNA molecule.

The variable changes $x_n=(u_n+w_n)/\sqrt{2}$ and $y_n=(u_n-w_n)/\sqrt{2}$ separate the Hamiltonian into in-phase and out-of-phase components. Only the out-of-phase motion stretches the hydrogen bond. The Hamiltonian for out-of-phase motion leads to an equation of motion

$$m\partial^2 y_n/\partial t^2-k(y_{n+1}+y_{n-1}-2y_n)^2 -2\sqrt{2}Da\exp(-\sqrt{2}ay_n)[\exp(-\sqrt{2}ay_n)-1]=0\ . \tag{3}$$

All figures shown were generated by time stepping through the integration of the full equations of motion for the connected chains using a fifth-order Runga-Kutta method.[12] For cases where the initial conditions are symmetric between the top and bottom chains, this is equivalent to solving the in-phase equation of motion, Eq. (3). Energies were calculated directly from the model and were conserved in all cases (except the random noise cases discussed below) to better than 0.001%. The

 

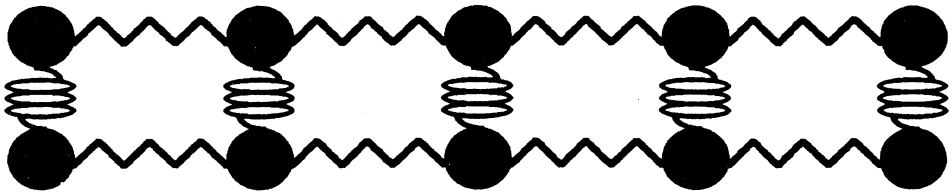

FIG. 1. Simple model of DNA with nonlinear interchain connections.

masses are constrained to move only in the vertical direction and the ends of the chains were left free in order to more accurately reflect biological conditions. The effect of also including longitudinal motion has been examined recently by Muto, Lomdahl, and Christiansen.[8]

## III. SOLUTIONS AND STABILITY

Remoissenet[11] has shown that the Hamiltonian (1) above leads, in leading nonlinear order and using a multiple-scale expansion method, to a nonlinear Schrödinger equation with discrete breather solitary waves of the form

$$y_n(t)=\epsilon A\ \mathrm{sech}\chi\cos(Kn\ell-\Omega t)-2\alpha\epsilon^2A^2\mathrm{sech}^2\chi + (\alpha A^2\epsilon^2/3)\mathrm{sech}^2\chi\cos[2(Kn\ell-\Omega t)]\ , \quad (4)$$

where

$$A=[(u_e^2-2u_eu_c)/2PQ]^{1/2}\ , \quad (5a)$$

$$\chi=\epsilon(n\ell-V_et)/L_e\ , \quad (5b)$$

$$\Omega=(\epsilon u_e/2P)(V_g+\epsilon u_c)^{1/2}+\omega\ , \quad (5c)$$

$$K=\kappa+\epsilon(u_e/2P)\ , \quad (5d)$$

$$P=(k\ell^2/2m\omega)[\cos(\kappa\ell)-(k/m\omega^2)\sin^2(\kappa\ell)]\ , \quad (5e)$$

$$Q=(\omega_0^2/2\omega)\{4\alpha^2-2\alpha^2/[3+(16k/m\omega_0^2)\sin^4(\kappa\ell/2)] -3\beta\}\ , \quad (5f)$$

$$\omega^2=\omega_0^2+4(k/m)\sin^2(\kappa\ell/2)\ , \quad (5g)$$

$$\omega_0^2=4Da^2/m\ , \quad (5h)$$

$$\alpha=-6\sqrt{2}a/\epsilon\ , \quad (5i)$$

$$\beta=7a^2/3\epsilon^2\ . \quad (5j)$$

Here $V_g=(k\ell/m\omega)\sin(\kappa\ell/2)$ is the group velocity, $L_e=2P/(u_e^2-2u_eu_c)^{1/2}$, is the breather width, $\ell$ is the lattice spacing, $\kappa$ is the linear carrier wave vector, $u_e$ is the envelope velocity, $u_c$ is the carrier wave velocity and $\epsilon$ is an arbitrary scaling parameter which controls the (coupled) amplitude and width of the breather. The parameters $a$, $D$, and $k$ determine the strength of the coupling.

The numerical simulation used these solutions as initial conditions and found them to be reasonably stable for a wide range of coupling parameters including the biologically significant values $D=0.33$ eV, $a=1.8$ Å$^{-1}$ in the Morse potential and linear spring constant $k=0.003$ eV/Å$^2$. Values examined ranged from 10 to 0.5 for $a$; 10 to 0.2 for $D$ and 20 to 0.003 for $k$. It is important physically that for the biological parameters quoted above the breathers are very narrow and discrete lattice pinning effects are expected.[13] Pinning was seen in our simulations and for this reason slightly larger values of the parameters were chosen for most of the simulations so that effects not dominated by pinning could be examined. It remains to be seen whether discreteness effects will ultimately dominate biological conditions in realistic potentials and environments.

Equation (3) is not integrable in closed form with the result that the anharmonic phonons described by Eq. (4) are not true solitons and decay into other modes eventually. The amplitude of the breathers describe in this paper decreases by approximately 25% over a time interval of 100 time units (10 000 steps at intervals of 0.01).

The adjustable parameter $\epsilon$ in Eq. (4) determines the maximum amplitude and also the width of the initial breather. The masses in the chain were launched with velocities corresponding to derivatives of their position and as a consequence, $\epsilon$ also has some effect on the velocity of the moving breather. The Morse potential can be expanded for small $y$ as

$$-2\sqrt{2}Da\exp(-\sqrt{2}ay_n)[\exp(-\sqrt{2}ay_n)-1] =4Da^2y_n-6\sqrt{2}Da^3y_n^2+(28/3)Da^4y_n^3\ . \quad (6)$$

When the amplitude is increased to the point that the first nonlinear term in the expansion 15% of the linear term, the breather does not maintain its initial shape but radiates energy, settling into a quasistable breathing shape different from the initial one. For $\epsilon$ resulting in amplitudes which cause the first nonlinear term to exceed roughly 25% of the linear term, the breather splits into two breathers traveling in opposite directions (Fig. 2).

The carrier wave vector, $\kappa$, controls the shape of the breather. For the case $0<\kappa<1$, coefficients in the nonlinear Schrödinger equation are in the correct range for a breather solution.[14] Other signs and values of $\kappa$, giving rise to other types of nonlinear pulses such as "dark" solitons, asymmetric envelopes etc., were not examined.

The parameter $\kappa$ also has the largest effect on the velocity of the breather. Initial velocities were determined from derivatives of the initial positions of the masses. Because the expression for the velocities is not symmetric about the center of the breather, breathers cannot be launched with zero velocity. Larger values of $\kappa$ (with the

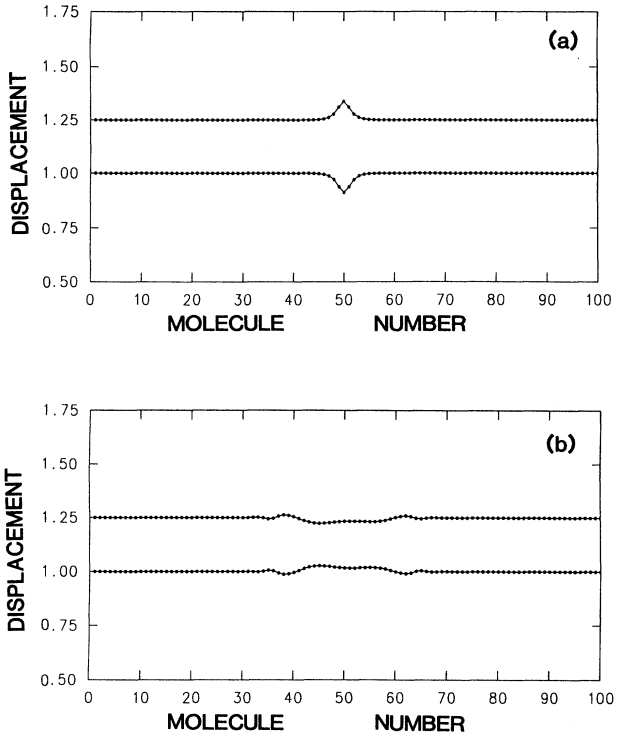


FIG. 2. A nearly stationary breather as an initial condition (a) and at 48 time units (b) showing the splitting in the case of large initial amplitude. Displacement represents the displacement of the top, $u$, and bottom, $w$, chains from equilibrium with an arbitrary equilibrium separation of 0.25. Parameter values are $k=1.0$, $\kappa=0.1$, $D=1.0$, $m=1.0$, $a=1.5$, and $\epsilon=0.2$.

restriction $0<\kappa<1$) cause more initial velocity asymmetry and therefore greater breather speeds along the chain.

Stability of the breathers was tested upon the introduction of random noise both as a simple initial condition and also in the case of continuous application of random noise. In the case of initial random noise, the breathers were as stable as nonperturbed initial conditions. This was true up to the point where random noise began to mask the breather shape. Energy was conserved in all of these cases. Stability was also tested for the introduction of random noise every 20 time steps, approximately representing a chain in contact with a thermal bath. A quantitative measure of stability is difficult but in these cases the breathers appeared quite stable for reasonably long time runs, typically 100 time units. Energy was not conserved exactly in these trials. The effects of thermal noise on single and double chains has been extensively examined by Muto, Lomdahl, and Christiansen.[8]

## IV. SINGLE MASS DEFECTS

Mass inhomogeneities along the DNA molecule due to the base pair sequence are small, constituting a variation of less than 13%.[1] This may however be deceptive in regard to the importance of examining mass defects along the chain. Although open and closed states can be seen in DNA and RNA molecules in the absence of other molecules, replication processes depend on the interaction of the DNA with large proteins called DNA polymerases.[1] These proteins wrap around the DNA chain covering up to 70 base pairs of the chain. The polymerase molecule does not bind equally strongly to each base pair so that the effect could be similar to large, varying mass defects along the chain. Assuming the mass of the polymerase to be distributed equally along 70 base pairs could amount to a mass defect of as much as 15 times the pair mass per base pair.

In order to examine the role of large mass defects along the chain, single mass defects varying between 0.25 and 4 times the original mass were placed at the center of a breather and the time evolution was followed. Any defect greater than approximately $\pm 10\%$ of the original mass was a sufficient disturbance to cause the breather to split up relatively quickly (Fig. 3). Breathers with defects less than approximately 5% appeared to be stable for the time scales examined.

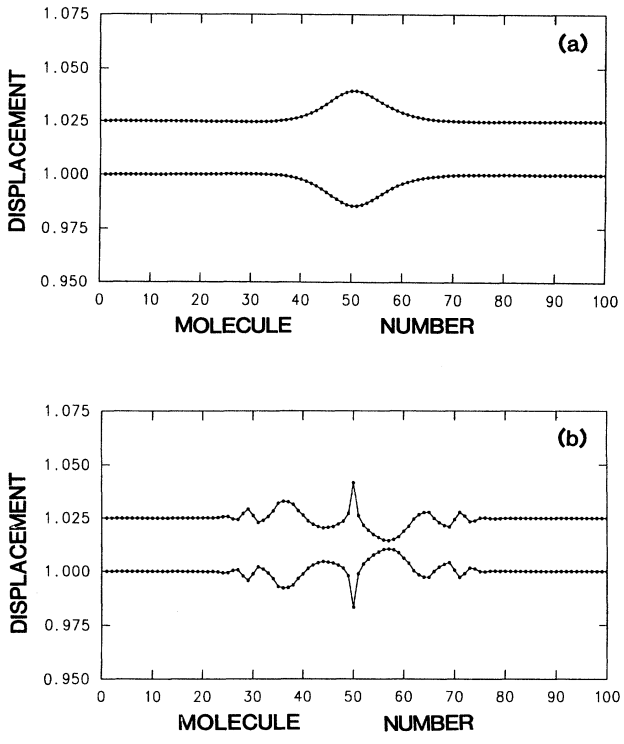


FIG. 3. A nearly stationary breather as an initial condition (a) and at 74 time units (b) showing breakup due to a mass defect of $m=4$ located at the center of the chain. Displacement represents the displacement of the top, $u$, and bottom, $w$, chains from equilibrium with an arbitrary equilibrium separation of 0.25. Parameter values are $k=1.0$, $\kappa=0.1$, $D=1.0$, $m=1.0$, $a=1.5$, and $\epsilon=0.01$.

A more quantitative approach for examining the relationship between linear defect modes and breather modes is to calculate single-particle velocity power spectrums. This was done using the maximum entropy method[12] to find the single particle power spectrum of the center (defect) mass on the chain. Linear theory predicts for a single mass defect in a linear discrete chain with free boundary conditions that lighter defects will give rise to discrete (local mode) frequencies above the band of (extended) normal modes.[15]

Assuming the (linear) coupling to be complicated enough (more than one linear coupling or second nearest-neighbor interaction) so that the normal mode band does not extend to zero frequency, heavier defects will give rise to frequencies below the band. For only nearest-neighbor linear interactions, the heavier impurity modes occur in the band as resonances. The band of linear normal mode frequencies for a linearized Morse potential is given by

$$\omega=[(k/m)(\lambda-2\cos\phi)]^{1/2}\ , \tag{7}$$

where $\lambda=2+4Da^2/k$.

Linear modes for single mass defects on the double-chain system were examined by displacing a single mass defect by a small distance and finding the single-particle frequency spectrum.

Frequencies for breathers without defects were found to lie within the linear band of normal modes. When single mass defects were added to the breather, there was some interaction of modes as can be seen in Table I. Starred values are the larger of the pair when two frequencies were observed.

The following interpretation seems plausible. For lighter mass defects, the linear defect modes appear along with the breather mode with both shifted slightly downwards in frequency. It would thus seem that breathers with the lighter defect frequency do not exist. For the case of a heavier mass defect, the breather frequencies become locked with the defect frequency for any significant mass defect. Evidently breathers with frequencies equal to heavier mass defect frequencies are available. This is in agreement with arguments presented in a paper by Kosevich and Kovalev for a one-dimensional model of the Frenkel-Kontorova type.[16] They examine anharmonic localized modes and the effect on them by isotopic defects and conclude that a finite minimum energy is needed to excite a self-localized mode near a light impurity but not near a heavy defect. Identical calculations can be carried out for the present-double chain system showing, at least in the continuum approximation, that a finite minimum energy is needed for light impurity local modes to exist but not heavy impurity local modes. Minimum energies calculated for light defect impurity modes in a continuum approximation fall well above predicted breather energies in the present model, so that a single localized mode containing both breather and light impurity is not possible.

## V. MULTIPLE MASS DEFECTS

Multiple mass defects of two times the original mass were placed on both top and bottom chains for varying lengths of chain with a breather centered on the defect region. Uncentered mass defects covering half of a breather were also studied. In all of these cases the energy of the portion of the breather originally inside the defect region remained trapped in the region (Fig. 4). Trapping due to discreteness effects has been excluded in this and all of the following cases by the choice of parameters $a=1.5$, $D=1.0$, and $k=1.0$.

Multiple mass defects of varying magnitude (50 to 0.5 times the original mass) were placed along a 40 mass length of chain with a breather centered in the defect region. For defects greater than twice and less than half the original mass, the breather remained trapped in the defect region, bouncing back and forth between the boundaries of the region with very little energy transmitted outside of the region. This is in agreement with the results of Techera, Daemen, and Prohofsky.[10] For regions with weaker defects (defect mass ratios 0.5 to 2) the breather was not trapped. Some reflection of energy and some modification of breather shape was noticed when the breather penetrated these weaker defect regions (Fig. 5). The value of $\epsilon$ (and therefore the amplitude) did not appear to change the trapping of the breather in defect regions up to amplitudes large enough to cause breakup.

Breathers were also launched on chains with 40 con-

TABLE I. Single-particle vibrational frequencies of the center defect mass in the chain for small amplitude (linear) vibrations and for breather plus defect.

| Mass ratio | ($f$) linear defect | ($f$) breather plus defect |
|---|---|---|
| 0.85 | 0.6050 | 0.4820* and 0.6010 |
| 0.90 | 0.5880 | 0.4820* and 0.5850 |
| 0.95 | 0.5880 | 0.4890 |
| 0.98 | 0.4550 and 0.5830* | 0.4900 |
| 1.00 (no defect) | 0.4650 and 0.5760* | 0.4900 |
| 1.02 | 0.4850 and 0.5720* | 0.4880 |
| 1.05 | 0.4870* and 0.5660 | 0.4860 |
| 1.10 | 0.4790 | 0.4770 |
| 1.15 | 0.4640 | 0.4630 |

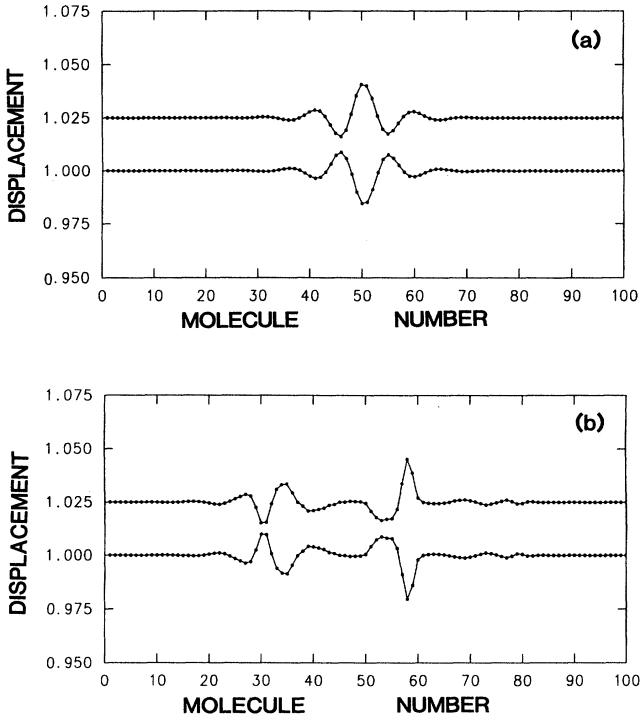


FIG. 4. Trapping of a portion of a moving breather in a defect region. Mass defects of $m=2$ are loaded on both chains from mass 50 to 60. (a) is initial condition and (b) is at 70 time units. Displacement represents the displacement of the top, $u$, and bottom, $w$, chains from equilibrium with an arbitrary equilibrium separation of 0.025. Parameter values are $k=1.0$, $\kappa=0.95$, $D=1.0$, $m=1.0$, $a=1.5$, and $\epsilon=0.01$.

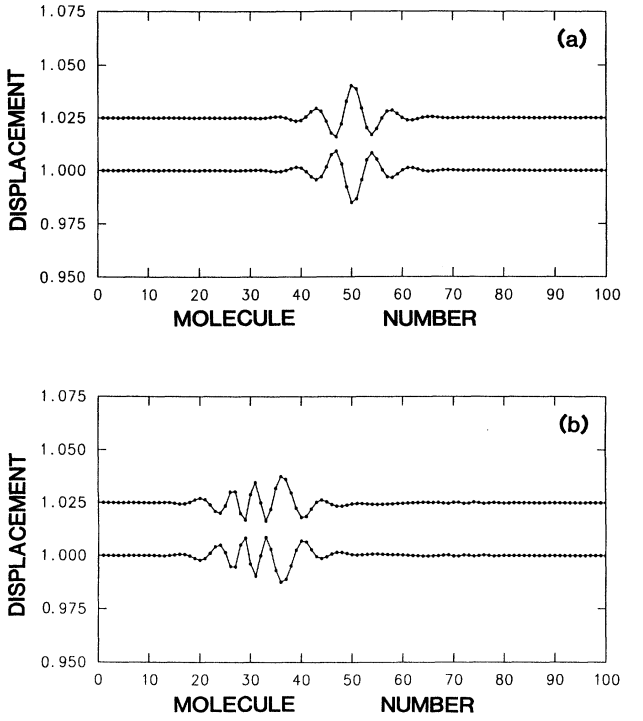


FIG. 5. Penetration of a moving breather from an area of slighter defects into a region of no mass defects. Defects of $m=1.1$ are on both chains from mass number 25 to 35. (a) is initial condition and (b) is at 78 time units. Displacement represents the displacement of the top, $u$, and bottom, $w$, chains from equilibrium with an arbitrary equilibrium separation of 0.025. Parameter values are $k=1.0$, $\kappa=0.95$, $D=1.0$, $m=1.0$, $a=1.5$, and $\epsilon=0.01$.

secutive mass defects of 2 and 0.5 times the original mass only on the top chain. In these cases a breatherlike wave with a modified shape remained trapped in the defect region and a low amplitude pulse of greater (linear) speed with almost no interchain stretching was expelled from both sides of the defect region (Fig. 6).

A sinusoidally varying mass defect of $m[1+0.1\sin(\omega x)]$ was also placed on the chain with a breather as initial conditions. When the wavelength of the defect region is much smaller than the width of the breather, the breather remains stable with small changes in its structure. A defect region of large wavelength relative to the breather width will also result in stable breathers with a coherent "particle like" motion, well described by perturbation theory or energy arguments. In the intermediate regime, where the defect region wavelength is of the same order as the breather width, there is a modification of the breather shape. In this case the breather oscillates irregularly between several stable shapes (Fig. 7). This intermediate regime is difficult to describe analytically and is perhaps the most qualitatively significant effect of combining disorder and nonlinearity.

Sinusoidally varying defect regions of large wavelength with smaller variances $m[1+0.01\sin(\omega x)]$ do not trap moving breathers, whereas regions with larger defects $m[1+0.1\sin(\omega x)]$ do trap breathers (Figs. 8 and 9). As the breather propagates some energy shifts periodically between potential and kinetic energy while maintaining constant total energy. For defects of $\pm 0.01$ this variation in energy from kinetic to potential is larger than the total energy difference between regions with defects of $+0.01$ m and regions of $-0.01$ m. For defects of $\pm 0.1$ m the variation in energy from kinetic to potential is smaller than the total energy difference between regions with defects of $+0.1$ and $-0.1$ m. Thus breathers have the required energy for propagating into weak mass defect regions but not into strong defect regions. It is also interesting to note that the breathers remain trapped in regions of higher mass (and therefore higher energy) but break up when initially placed in regions of lower mass. This is the opposite of what might be expected and is possibly due to the absence of appropriate energies for breathers in the lighter regions which start out with energies corresponding to a heavier region, as in the case of single mass defects discussed above.

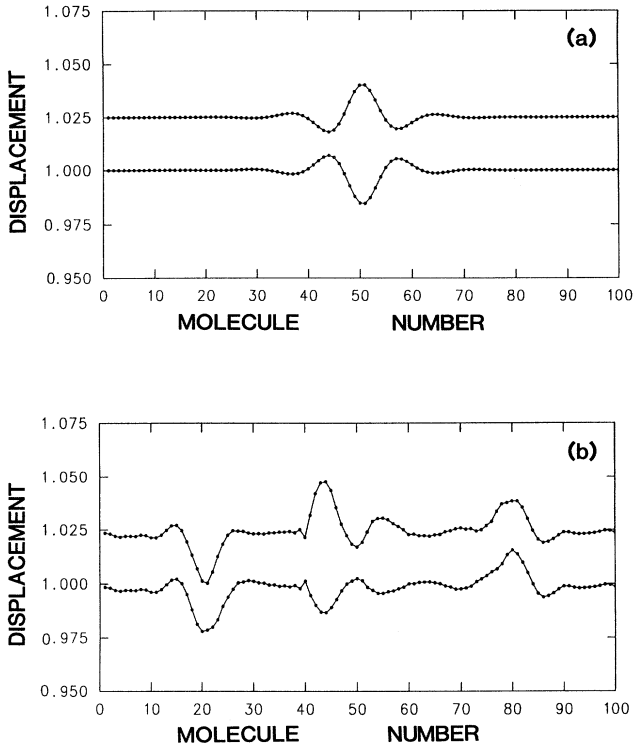


FIG. 6. A moving breather placed on a chain with mass defects of $m=0.5$ only along the top chain at time zero (a) and 70 time units (b). Displacement represents the displacement of the top, $u$, and bottom, $w$, chains from equilibrium with an arbitrary equilibrium separation of 0.025. Parameter values are $k=1.0$, $\kappa=0.5$, $D=1.0$, $m=1.0$, $a=1.5$, and $\epsilon=0.01$.

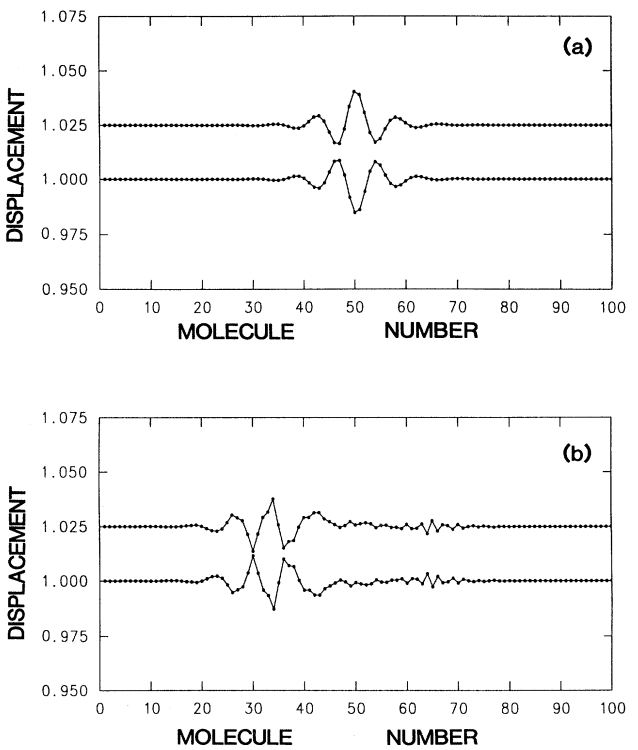


FIG. 7. Breather moving in a small wavelength, sinusoidally varying mass defect of $m=1.0+0.1\sin(3x)$ at initial (a) and 84 time steps (b). Displacement represents the displacement of the top, $u$, and bottom, $w$, chains from equilibrium with an arbitrary equilibrium separation of 0.025. Parameter values are $k=1.0$, $\kappa=0.95$, $D=1.0$, $m=1.0$, $a=1.5$, and $\epsilon=0.01$.

## VI. CONCLUSION

The stability of discrete breather solutions representing open states on a two chain model of DNA with a Morse potential for interchain coupling was examined numerically. Breather solutions were found to exist for coupling parameter values believed to be of biological significance. For these values discrete lattice pinning effects predominate. The majority of the simulations were performed with slightly larger parameter values in order to examine effects not dominated by pinning.

Stability of the breather solutions was tested under conditions of initial random noise and also conditions of periodically applied random noise. In both cases the breathers were found to be stable over long time spans for moderate amounts of noise.

Single-particle frequency spectrums were examined for cases of single mass defects added to the chain. Large single defects either smaller or larger than the original masses caused the breather to break up. Smaller single mass defects which have magnitudes less than the original mass were found to form separate discrete frequencies in addition to the breather frequencies. Small defects with magnitudes larger than the original mass couple with the breather to form discrete frequencies lower than the defect-free breather.

Cases of multiple mass defects were also examined. Breathers were found to be trapped in defect regions which are wider than the initial breather. Breathers were also found to be trapped in regions where the mass defects varied sinusoidally with large wavelength by $\pm 0.1$ m but were not trapped in regions where the defects varied by $\pm 0.01$ m. For sinusoidally varying defect regions with wavelength smaller than the breather width, the breathers were not trapped.

Real DNA molecules and their interactions with their environment are vastly more complicated than a simple mass chain model can represent. Longitudinal motion along the chain and effects of the secondary structure of DNA, for example, has not been included here. However, it is clear that nonlinear self-focusing of energy provides a possible mechanism for the initiation of open states of DNA involved in melting and replication processes. It is also interesting to note from the present results that self-localized coherent states are affected by small mass defects and in fact cannot be sustained in the

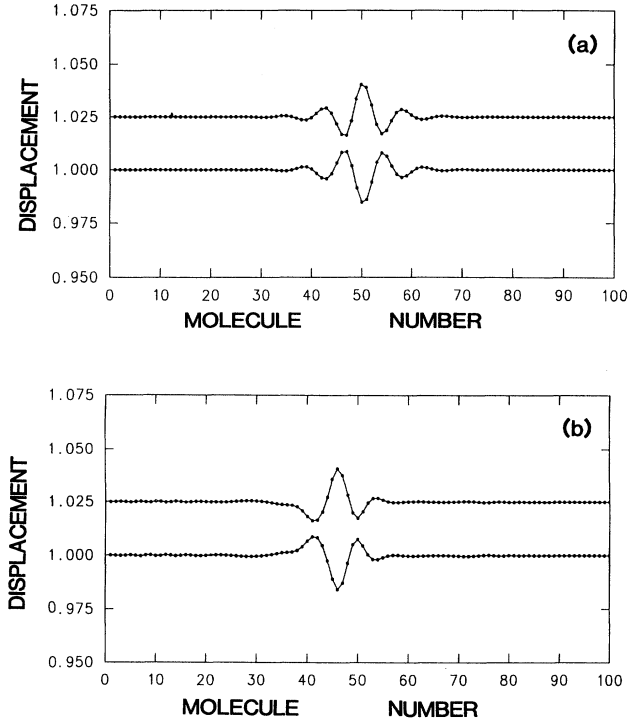


FIG. 8. Moving breather trapped in a long wavelength, sinusoidally varying mass defect of $m=1.0+0.1\sin(0.16x)$ at initial (a) and 96 time units (b). Displacement represents the displacement of the top, $u$, and bottom, $w$ chains from equilibrium with an arbitrary equilibrium separation of 0.025. Parameter values are $k=1.0$, $\kappa=0.95$, $D=1.0$, $m=1.0$, $a=1.5$, and $\epsilon=0.01$.

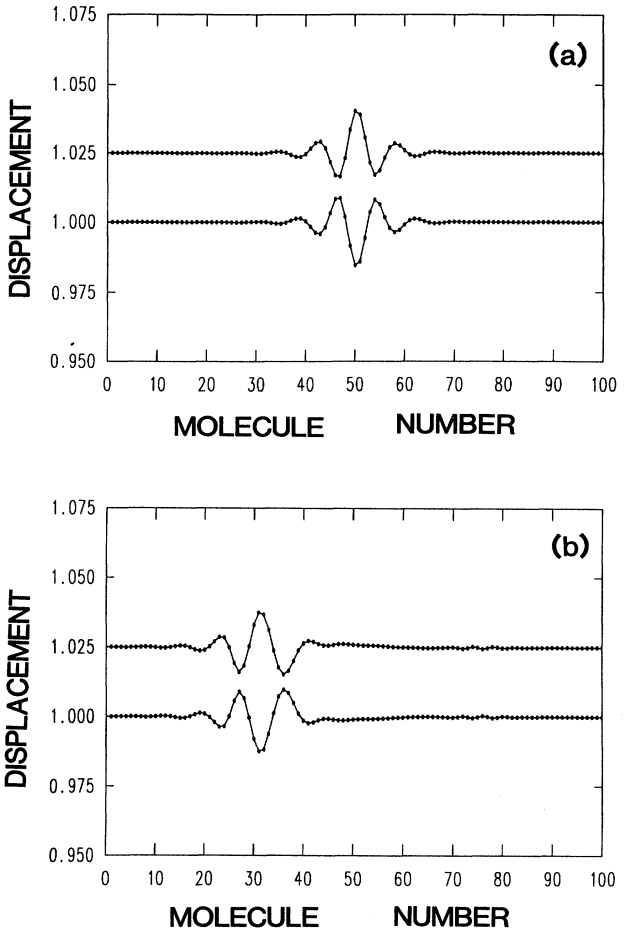


FIG. 9. Moving breather not trapped in a long wavelength, sinusoidally varying mass defect of $m=1.0+0.01\sin(0.16x)$ at initial (a) and 86 time units (b). Displacement represents the displacement of the top, $u$, and bottom, $w$, chains from equilibrium with an arbitrary equilibrium separation of 0.025. Parameter values are $k=1.0$, $\kappa=0.95$, $D=1.0$, $m=1.0$, $a=1.5$, and $\epsilon=0.01$.

presence of large defects. Thus a mechanism exists whereby small inhomogeneities representing genetic coding can affect the dynamics of opening and closing of the double-chain system. The present model is thus a step towards understanding some of the nonlinear dynamics which may be occurring along the chain during or preceding the processes of chain opening and closing

## ACKNOWLEDGMENTS

One of us (K.F.) is grateful for support from the Theoretical Division and Center of Nonlinear Studies, Los Alamos National Laboratory, where most of this work was performed. Work at Los Alamos is performed under the auspices of the U.S. Department of Energy (USDOE).

[1]B. Alberts, D. Bray, J. Lewis, M. Raff, K. Roberts, and J. D. Watson, *Molecular Biology of the Cell* (Garland, New York, 1983).
[2]E. W. Prohofsky, Phys. Rev. A **38**, 1538 (1988).
[3]S. W. Englander, N. R. Kallenbach, A. J. Heeger, J. A. Krumhansl, and S. Kitwin, Proc. Nat. Acad. Sci. U.S.A. **777**, 7222 (1980).
[4]S. Yomosa, Phys. Rev. A **27**, 2120 (1983); **30**, 474 (1984).
[5]S. Takeno and S. Homma, Prog. Theor. Phys. **77**, 548 (1987).
[6]Chung-Ting Zhang, Phys. Rev. A **35**, 886 (1987).
[7]M. Peyrard and A. R. Bishop, Phys. Rev. Lett. **62**, 2755 (1989).
[8]V. Muto, P. S. Lomdahl, and P. L. Christiansen Phys. Rev. A **42**, 7452 (1990).
[9]V. Muto, A. C. Scott, and P. L. Christiansen (unpublished).
[10]M. Techera, L. L. Daemen, and E. W. Prohofsky (unpublished).

[11]M. Remoissenet, Phys. Rev. B **33**, 2386 (1986).
[12]W. H. Press, B. P. Flannery, S. A. Teukolsky, and W. T. Vetterling, *Numerical Recipes* (Cambridge University Press, Cambridge, England, 1989).
[13]J. F. Currie, S. E. Trullinger, A. R. Bishop, and J. A. Krumhansl, Phys. Rev. B **15**, 5567 (1977).
[14]S. Pnevmatikos, N. Flytzanis, and M. Remoissenet, Phys. Rev. B **33**, 2308 (1986).
[15]R. F. Wallis and A. A. Maradudin, Prog. Theor. Phys. **24**, 1055 (1960).
[16]A. M. Kosevich and A. S. Kovalev, Fiz. Nizk. Temp. **1**, 1544 (1975) [Sov. J. Low Temp. Phys. **1**, 742 (1975)].